

Compact Surjective Encoding Autoencoder for Unsupervised Novelty Detection

Jaewoo Park, Yoon Gyo Jung, and Andrew Beng Jin Teoh

Department of Electrical and Electronic Engineering, Yonsei University
{julypraise, jungyg, bjteoh}@yonsei.ac.kr

Abstract. In unsupervised novelty detection, a model is trained solely on the in-class data, and infer to single out out-class data. Autoencoder (AE) variants aim to compactly model the in-class data to reconstruct it exclusively, differentiating it from out-class by the reconstruction error. However, imposing compactness improperly may damage in-class reconstruction and, therefore, detection performance. To solve this, we propose Compact Surjective Encoding AE (CSE-AE). In this model, the encoding of any input is constrained into a compact manifold by exploiting the deep neural net's ignorance of the unknown. Concurrently, the in-class data is surjectively encoded to the compact manifold via AE. The mechanism is realized by both GAN and its ensembled discriminative layers, and results to reconstruct the in-class exclusively. In inference, the reconstruction error of a query is measured using high-level semantics captured by the discriminator. Extensive experiments on image data show that the proposed model gives state-of-the-art performance.

Keywords: Unsupervised Novelty Detection, Generative Adversarial Network

1 Introduction

Novelty detection is a task to detect an incoming signal that deviates from the underlying regularity of a known class [1]. *Unsupervised* novelty detection, in particular, assumes that only the known, *in-class* samples are available for training. In the inference stage, the trained system needs to detect *out-class* instances, differentiating them from the in-class data. Due to the absence of out-class knowledge, the problem is highly challenging. The range of unsupervised novelty detection application is diverse from medical data processing [49,57,56] to intruder detection [46,43], abnormality detection [55], and fraud detection [70]. Moreover, novelty detection has a deep root in neuroscience [62,30,14] as it constitutes the core neural mechanism of intelligent beings [60].

Many successful methods in unsupervised novelty detection follow one of the following two approaches. In the first strategy, a density function of the in-class data is modeled, and then a query located on the low-density region is classified as out-class [15,2,36,28,52]. The second strategy is by reconstruction-based methods [26,8,54,45], the core principle of which is to design a mapping

that is invertible exclusively over the in-class manifold. To differentiate in-class and out-class samples, the models often come together with a score function that measures the novelty of a query, which can be sample-wise reconstruction loss used in the training of their models [54], a score derived by an independent module [53,45], or a mixture of them [1].

As to the reconstruction-based approach, most of the models follow the paradigm of compact representation learning [18] to acquire a function that reconstructs the in-class data only. Its latent representations are learned to be compact in the sense that they are so condensed as to represent the in-class data exclusively. For example, principal component analysis (PCA)-based methods [5,26,8] select a minimal number of eigen-axes by which to reconstruct the in-class data. The recent advances in deep learning [32,21] enabled the reconstruction-methods to seek compact representations in more diverse manners. Deep auto-encoder (AE) achieves this goal by making its middle layer much lower-dimensional than its input dimension and thereby posing a bottleneck therein. Moreover, progresses in generative adversarial learning [17] enabled AE to constrain its latent representations in a pre-specified bounded region [45], showing promising results.

However, imposing compactness on the latent representations of AE in an improper way might collapse the encodings and, in turn, the in-class reconstruction deteriorates, thereby failing the novelty detection system. Moreover, practical AE cannot perfectly reconstruct an in-class query; it can only be that the reconstruction-error is smaller over the in-class than over out-class, and in fact it is smaller only if they are measured by a proper metric.

To this end, we propose CSE-AE (Compact Surjective Encoding Autoencoder), a novel model with a theoretical guarantee for reconstructing in-class data exclusively. In CSE-AE, the encoding of any input is constrained into a compact manifold. To which, the in-class data is surjectively encoded and, then, decoded to reconstruct it. For realization, we propose several techniques based on generative adversarial network (GAN) [17]. Specifically:

- To realize CSE-AE, firstly, we *constrain* the encoding of any input into a compact manifold. This is done by GAN and exploiting the characteristic that deep neural network (DNN) does not distinguish between the known and the unknown.
- Secondly, to encode the in-class data *surjectively* onto the compact manifold, we adversarially enforce every latent point to represent an in-class sample.
- Finally, to ensure robust reconstruction of the in-class samples, we reconstruct through their projections from the *ensembled* layers of the input discriminator in the GAN. Concurrently, every encoding point is also reconstructed, which is to ensure reconstruction of generated in-class samples.
- For inference, the reconstruction error is measured based on the *penultimate* feature of the input discriminator. In the space of this feature, the in-class is (linearly) separated from the *badly* generated in-class samples, which are effective representatives of out-class.

We highlight that our problem to solve in this work is *fully unsupervised* (one-class) novelty detection. There are other, different settings for novelty de-

tection: for example, semi-supervised novelty detection [51,23] allows to train with out-class data, and self-supervised novelty detection [16,24] allows a model to exploit supervisory signals inferred from a simple rule. Both settings require some amount of expert knowledge and/or human prior on a given training data. (For further discussion, see Supplementary Sec. 1.) In our unsupervised setting, we only assume that a given training data set is one-class (i.e., the known class).

2 Related Work

An extensive amount of research has been conducted on novelty detection, often called by other names such as one-class classification [58] or anomaly detection [10]. Many of the recent unsupervised novelty detectors employ density estimation and/or reconstruction-based approach but not all of them [50,42,19] fall in these categories. For a general survey, readers are recommended to refer [10,48].

Reconstruction-based Approaches. The practice of reconstruction-based methods in unsupervised novelty detection dates back to PCA [5], and its kernel version [26] applicable to non-gaussian data, and a later variant Robust PCA [8] that resolves the outlier sensitivity of the vanilla PCA. Another line of work uses sparse coding [69,13] to project the in-class data onto the low-dimensional subspace, assuming that this subspace can capture the in-class data in a compact way. The reconstruction error for these methods is defined as the discrepancy made by the subspace projection.

The recent advance in representation learning [4] by deep neural network enabled dimensionality reduction using autoencoder [20] with a convolutional neural network (CNN) architecture having a bottleneck on its middle layer. [54] applied this notion to compactly model the in-class data for unsupervised novelty detection, followed by other variants [11,9]. In [54], however, the reconstruction error defined by Euclidean distance suffers from the curse of dimensionality, and the high capacity of the neural network does not prevent out-class samples to be finely reconstructed.

With the progress in generative modeling, [3] applied variational autoencoder (VAE) [29] to manifest reconstruction error probabilistically, but due to its model design the density is confined to be a specific distribution. [57] and its later version [56] applied GAN to model the in-class data. Without an encoder, [57] reconstructs a query by searching a corresponding latent vector with backpropagation.

More recently, the reconstruction-based method has been combined with density estimation approach in [47,1]. [47] models the in-class manifold into a latent space by means of adversarial autoencoder (AAE) [37] with an additional discriminator. The density of an input is empirically approximated as the product of two marginals which are parallel and orthogonal, respectively, to the tangent space. [1], on the other hand, estimates the density of the latent vector using an autoregressive estimator, and defines the novelty score as a combination of reconstruction error and the negative log-likelihood.

The recent AE-based models [53,45] are more explicitly oriented to compact representation learning. In [53], the AE output of every noisy in-class sample is constrained into the in-class manifold. On the other hand, in [45], the encoding output of any input vector is constrained into a unit cube. For [45], the mechanism is realized by both GAN and using tanh activation on the final layer of the encoder. However, constraining as such might collapse latent representation and the decoder’s generative quality as reported in [45]. The work mitigates this issue by informative-negative sampling. However, on a complex dataset such as CIFAR-10 [31], it does not significantly outperform other previous methods, leaving room for improvement.

3 Method

Compact surjective encoding via AE (CSE-AE) is a general model that aims to reconstruct the in-class data exclusively. In this section, we first introduce this framework and, subsequently, propose techniques to realize it.

Before initiating, we define few notations: Our autoencoder consists of an encoder $E = E(\cdot; \theta_E)$ and a decoder $G = G(\cdot; \theta_G)$ parametrized by θ_E and θ_G , respectively. The input space $\mathcal{X} \subseteq \mathbb{R}^d$ consists of the in-class data \mathcal{X}_{in} and out-class $\mathcal{X}_{out} = \mathcal{X} \setminus \mathcal{X}_{in}$. In-class $\mathbf{x}_{in} \in \mathcal{X}_{in}$ denotes a sample or a variable depending on the context, and similarly for $\mathbf{x}_{out} \in \mathcal{X}_{out}$. $d(\mathbf{z}, \mathcal{M})$ denotes a distance between a point $\mathbf{z} \in \mathbb{R}^{d_z}$ and a compact manifold $\mathcal{M} \subseteq \mathbb{R}^{d_z}$. In our model, we assume \mathcal{M} is simply the d_z -dimensional closed hypercube: $\mathcal{M} = [-1, 1]^{d_z}$.

3.1 Compact Surjective Encoding via AE Model

In CSE-AE model, the encoding $E(\mathbf{x})$ of an arbitrary input $\mathbf{x} \in \mathcal{X}$ is *constrained* to a compact manifold \mathcal{M} (i.e., $E(\mathcal{X}) \subseteq \mathcal{M}$), and is *surjective* when its domain is restricted to the in-class data \mathcal{X}_{in} , (i.e., $E(\mathcal{X}_{in}) = \mathcal{M}$). Concurrently, the AE reconstructs all in-class data points: $\forall \mathbf{x}_{in}, G(E(\mathbf{x}_{in})) = \mathbf{x}_{in}$. In summary, the autoencoder in CSE-AE satisfies

$$E(\mathcal{X}) \subseteq \mathcal{M}, \quad E(\mathcal{X}_{in}) = \mathcal{M}, \quad \forall \mathbf{x}_{in} G(E(\mathbf{x}_{in})) = \mathbf{x}_{in}. \quad (1)$$

This AE reconstructs the in-class data exclusively since the AE reduces to identity function over \mathcal{X}_{in} and any out-class instance \mathbf{x}_{out} is mapped to an in-class sample \mathbf{x}_{in} through the AE. In information theoretic sense, the mutual information $I(\mathbf{x}_{in}, E(\mathbf{x}_{in}))$ is maximal while $I(\mathbf{x}_{out}, E(\mathbf{x}_{out}))$ deteriorates.

However, it is difficult to build such an AE. In the below, we propose techniques to approximately achieve this.

Remark OCGAN [45] also aims to achieve a similar goal. However, the encoding codomain of OCGAN is not compact and the encoding is not surjective. In fact, as they use tanh activation on the encoder output layer, the encoding outputs possibly collapse and disrupts the in-class reconstruction (i.e., $\mathbf{x}_{in} \neq G(E(\mathbf{x}_{in}))$) as experimentally found in their work. (For further discussion, see Supplementary Sec. 2.)

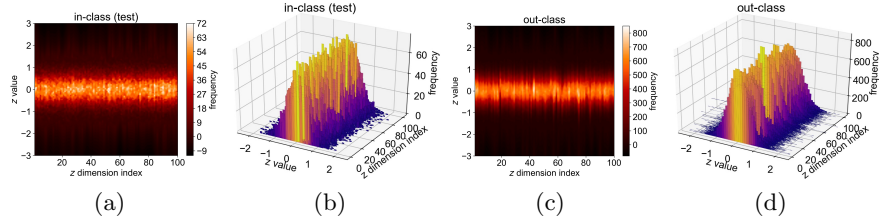


Fig. 1. Heat maps and histograms of scalar z_k along the dimension index k where $(z_1, \dots, z_k, \dots, z_{100}) = E(\mathbf{x}) \in \mathbb{R}^{100}$. For (a) and (b), $\mathbf{x} = \mathbf{x}_{in}$ are in-class test samples, and for (c) and (d) $\mathbf{x} = \mathbf{x}_{out}$ are out-class. The figures verify that not only \mathbf{x}_{in} but also \mathbf{x}_{out} are constrained into (or near to) $\mathcal{M} = [-1, 1]^{d_z}$ ($d_z = 100$).

3.2 Constrained Encoding by Deep Ignorance of the Unknown

It is widely known that conventionally trained deep neural network is unaware of the unknown. That is, a deep network cannot distinguish between \mathbf{x}_{in} and \mathbf{x}_{out} . To be precise, if a network is trained to minimize a loss function L on the training dataset from \mathcal{X}_{in} , then its *small loss open space*, which we define as

$$\{\mathbf{x} \in \mathcal{X}_{out} \mid L(\mathbf{x}) < \epsilon\} \text{ for small } \epsilon > 0, \quad (2)$$

is non-trivially large and close to \mathcal{X}_{in} . The phenomenon has been observed in distinct fields including adversarial attack [44,39], out-of-distribution detection [22,34,40], and open set recognition [6].

Though this characteristic is often regarded as a weakness of deep network, we exploit it to solve our problem. To constrain the encoding of *any* input $\mathbf{x} \in \mathcal{X}$ into \mathcal{M} , it is sufficient to constrain the encoding of the *in-class data only*. To this end, we apply the adversarial learning

$$\min_{\theta_E} \max_{\theta_{D_z}} L_{adv-z} = \frac{1}{N} \sum_{i=1}^N \log D_z(\mathbf{z}_i) + \log(1 - D_z(E(\mathbf{x}_i))). \quad (3)$$

Here, $D_z = D_z(\cdot; \theta_{D_z})$ is a latent discriminator, and $\{\mathbf{z}_1, \dots, \mathbf{z}_N\}$ and $\{\mathbf{x}_1, \dots, \mathbf{x}_N\}$ are batches sampled from the uniform prior $p_z(\mathbf{z}) = \mathcal{U}(\mathcal{M})$ and the in-class dataset \mathcal{X}_{in} , respectively. The output layer of E is *linearly activated* to optimize (3) properly.

Optimizing the adversarial loss in Eq. (3) enforces $E(\mathbf{x}_{in})$ to follow the prior $p_z = \mathcal{U}(\mathcal{M})$, and thus minimizes the distance $d(E(\mathbf{x}_{in}), \mathcal{M})$ between $E(\mathbf{x}_{in})$ and \mathcal{M} . We regard this distance as a loss function $L(\mathbf{x}_{in}) = d(E(\mathbf{x}_{in}), \mathcal{M})$ over \mathbf{x}_{in} that is minimized by training E . Then, since E does not distinguish between \mathbf{x}_{in} and \mathbf{x}_{out} as discussed in Eq. (2), $L(\mathbf{x}_{out}) = d(E(\mathbf{x}_{out}), \mathcal{M})$ would be low. In other words, \mathbf{x}_{out} is constrained to (or near to) \mathcal{M} . This property is verified by Fig. 1.

Remark It is sufficient to constrain \mathbf{x}_{out} close to the in-class. In general, it is easy to deteriorate the reconstruction of \mathbf{x}_{out} far away from the in-class.

3.3 Surjective Encoding of the In-Class by GAN

To enforce E to be surjective over \mathcal{X}_{in} , firstly, every encoding point $\mathbf{z} \in \mathcal{M}$ must represent an in-class data point (i.e., $G(\mathbf{z}) \in \mathcal{X}_{in}$), and secondly, the AE must reconstruct \mathcal{X}_{in} . That is:

Proposition 1 *If $G(\mathbf{z}) \in \mathcal{X}_{in}$ for all $\mathbf{z} \in \mathcal{M}$ and $\mathbf{x}_{in} = G(E(\mathbf{x}_{in}))$ for every $\mathbf{x}_{in} \in \mathcal{X}_{in}$, then $E : \mathcal{X}_{in} \rightarrow \mathcal{M}$ is surjective.*

To satisfy the first requirement in the sufficient condition in Proposition 1, we optimize the adversarial loss

$$\min_{\theta_G} \max_{\theta_{D_x}} L_{adv-x} = \frac{1}{N} \sum_{i=1}^N \log D_x(\mathbf{x}_i) + \log(1 - D_x(G(\mathbf{z}_i))) \quad (4)$$

Here, $D_x = D_x(\cdot; \theta_{D_x})$ is an input discriminator. Optimizing this adversarial loss minimizes the divergence $\text{KL}(p_{G(\mathbf{z})} \| p_{\mathbf{x}_{in}}) \rightarrow 0$, thereby mapping $G(\mathbf{z})$ into \mathcal{X}_{in} .

The second condition $\mathbf{x}_{in} = G(E(\mathbf{x}_{in}))$ in Proposition 1 will be sought by the subsequent technique.

3.4 Ensembled Reconstruction

The last part we need to satisfy to build CSE-AE is to ensure our AE to be reconstructive over \mathcal{X}_{in} , or more precisely, $G(E(\mathbf{x}_{in})) = \mathbf{x}_{in}$ for every in-class data sample \mathbf{x}_{in} . Attaining this requirement is problematic for two reasons: Firstly, the image \mathbf{x}_{in} is of high-dimensionality. Secondly, constraining the encoder by the adversarial loss in (1) may collapse the latent representation $E(\mathbf{z})$ because of the mode collapse issues in GAN.

As to the first reason, merely minimizing the L_2 distance $\|\mathbf{x}_{in} - G(E(\mathbf{x}_{in}))\|_2$ is not effective due to the curse of dimensionality. To resolve this, we reconstruct \mathbf{x}_{in} through the internal layers of the input discriminator D_x ; i.e., we minimize *ensembled adversarial feature loss*

$$L_{eaf}(\theta_E, \theta_G) = \frac{1}{N} \sum_{i=1}^N \sum_{l=0}^L \|f_l(\mathbf{x}_i) - f_l(\widehat{\mathbf{x}}_i)\|_1 \quad (5)$$

where $\widehat{\mathbf{x}}_i = G(E(\mathbf{x}_i))$, $f_l = f_l(\cdot; \widehat{\theta}_{D_x})$ is a hidden layer (i.e., a feature map) of D_x , $f_0(\mathbf{x}) := \mathbf{x}$, $\widehat{\theta}_{D_x}$ of f_l are the frozen copies of θ_{D_x} , and $L > 0$ is the number of the hidden layers selected in D_x . The features f_l capture the semantics that is somewhat coherent to that of human cognition [68], and that is diverse [67,66,27]. Thus, reconstructing through the ensembled adversarial features f_l induces a robust reconstruction of the in-class data. In Supplementary Sec. 3, we theoretically analyze how L_{eaf} is beneficial to our model both for training and inference.

Note that the training set $\{\mathbf{x}_1, \mathbf{x}_2, \dots\}$ is finite and, therefore, not dense in the whole in-class data \mathcal{X}_{in} . Thus, reconstructing real samples only may not

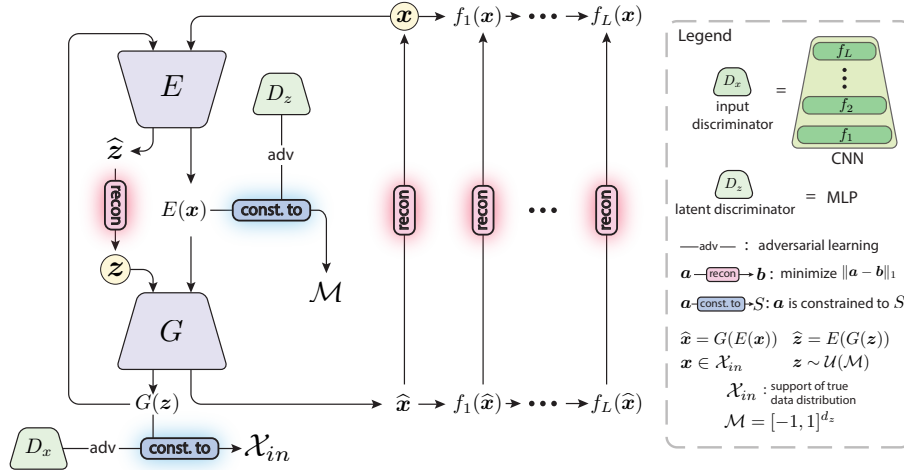


Fig. 2. A schematic diagram for our realization of CSE-AE.

be sufficient to guarantee the injectivity of $E : \mathcal{X}_{in} \rightarrow \mathcal{M}$. For this reason, we reconstruct over generated samples $G(z_i)$ as well. This is implicitly achieved by minimizing the *latent reconstruction* loss

$$L_{inv-z}(\theta_E, \theta_G) = \frac{1}{N} \sum_{i=1}^N \|z_i - \hat{z}_i\|_1 \quad (6)$$

where $\hat{z}_i = E(G(z_i))$. The following proposition shows that minimizing L_{adv-z} implies the reconstruction over the generated samples.

Proposition 2 For any $z \in \mathcal{M}$, $\|G(z) - \widehat{G(z)}\|_1 \leq \|G\|_{Lip} \|z - \hat{z}\|_1$ where $\widehat{G(z)}$ is the reconstruction of $G(z)$.

We note that the latent reconstruction loss L_{inv-z} directly counteracts the collapse issue caused by adversarially constraining the encoder output (i.e., the loss L_{adv-z} in Eq. (3)).

Overall, L_{eaf} together with L_{inv-z} form a modified cyclic loss [71].

3.5 Full Objective

The full objective to realize CSE-AE is to adversarially optimize

$$\min_{\theta_E, \theta_G, \theta_{D_z}, \theta_{D_x}} \max L_{adv-z} + L_{adv-x} + \alpha_x L_{eaf} + \alpha_z L_{inv-z}. \quad (7)$$

Here, the coefficients α_x and α_z control the contributions of the reconstructions in the input x and latent vector z , respectively. If α_x and α_z are too large, the model reduces to an autoencoder without a generative property.

The detailed algorithm of our CSE-AE is given in Supplementary Sec. 2, with its depiction in Fig. 2.

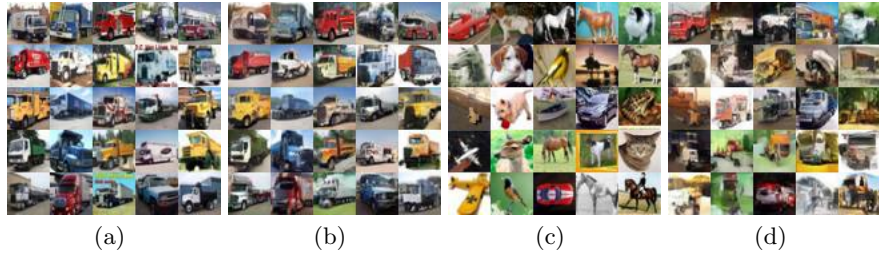


Fig. 3. Here, \mathcal{X}_{in} is the truck class in CIFAR-10, and \mathcal{X}_{out} is the rest of the classes. (a) test in-class \mathbf{x}_{in} , (b) test in-class reconstructions $\hat{\mathbf{x}}_{in}$, (c) out-class \mathbf{x}_{out} , (d) out-class reconstructions $\hat{\mathbf{x}}_{out}$.

Other Regularization We apply other regularizations which are crucial to the successful training of our model. (a) All networks (D_x , D_z , E , and G) are *spectral-normalized* [38] to stabilize the optimization of the adversarial losses. (b) The coefficients α_x and α_z linearly increase from 0 to their given values. This is to *synchronize* the reconstruction losses with the adversarial losses; adversarial learning is relatively slower than learning reconstruction.

3.6 Novelty Score

AE novelty detectors define novelty score by the reconstruction error. Since it is generally not possible to have the ideal condition $\mathbf{x}_{in} = G(E(\mathbf{x}_{in}))$, $\mathbf{x}_{out} \neq G(E(\mathbf{x}_{out}))$, carefully designing the measure of reconstruction error is crucial.

In fact, as seen in Fig. 3, our CSE-AE also does not reconstruct the in-class data perfectly (as the CSE-AE we trained is only an approximation of the ideal CSE-AE). However, the original in-class data samples \mathbf{x}_{in} and their reconstructions $\hat{\mathbf{x}}_{in}$ share the same class-semantics (Fig. 3(a)-(b)) while \mathbf{x}_{out} and $\hat{\mathbf{x}}_{out}$ do not (Fig. 3(c)-(d)). Thus, to effectively separate \mathbf{x}_{out} from \mathbf{x}_{in} by their reconstruction errors, we need a measure that captures class-semantics difference.

We argue that the penultimate layer f_L of the input discriminator D_x effectively serves this purpose. Firstly, it is widely agreed (and visually verified) that the deeper layers of a CNN capture higher-level semantics. Moreover, over the space of f_L , the in-class data \mathcal{X}_{in} is (linearly) separated from badly generated samples $G(\mathbf{z}_{bad})$ with $\mathbf{z}_{bad} \in \mathbb{R}^{d_z} \setminus \mathcal{M}$ and $D_x(G(\mathbf{z}_{bad})) < \min_{\mathbf{x}_{in} \in \mathcal{X}_{in}} D_x(\mathbf{x}_{in})$ because D_x is an adversarial discriminator. As seen in Fig. 4, such $G(\mathbf{z}_{bad})$ in fact exists and serves as out-class exemplars (i.e., has class-semantics different from that of the in-class). They are, however, not too distant from the in-class \mathcal{X}_{in} . This implies that the boundary that separates \mathcal{X}_{in} from out-class exemplars $G(\mathbf{z}_{bad})$ is tight to \mathcal{X}_{in} . Thus, over the space of f_L , there is a sharp distinction between \mathcal{X}_{in} and out-class.

Motivated by the above, we define a novelty score based on the *content loss* over f_L :

$$s_c(\mathbf{x}) = \|f_L(\mathbf{x}) - f_L(\hat{\mathbf{x}})\|_1. \quad (8)$$

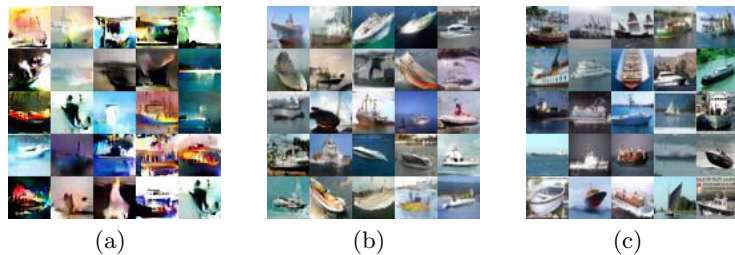


Fig. 4. Here, \mathcal{X}_{in} is the ship class in CIFAR-10. (a) badly generated samples $G(\mathbf{z}_{bad})$, (b) generated samples $G(\mathbf{z})$, (c) real in-class \mathbf{x}_{in} . The figures show that $G(\mathbf{z}_{bad})$ exist (i.e., can be sampled), represent out-class, but not too distant from \mathcal{X}_{in} .

Centered Co-activation Novelty Score Vast amount of literature in retrieval problem both experimentally [64,41] and theoretically [63] supports that angular distance better captures class-relation than L_p -distances. However, the angular distance does not capture minute details as well as L_1 . Thus, we'd like to benefit from both. To this end, we define *centered co-activation novelty score*

$$s_a(\mathbf{x}) = 1 - a(f_L(\mathbf{x}) - m(\mathbf{x}), f_L(\hat{\mathbf{x}}) - \hat{m}(\hat{\mathbf{x}})) \quad (9)$$

where $a(\mathbf{x}, \mathbf{y}) := \mathbf{x}^T \mathbf{y} / \|\mathbf{x}\|_2 \|\mathbf{y}\|_2$ is the cosine similarity, and $m(\mathbf{x})$ is the per-sample mean of $f_L(\mathbf{x})$, i.e., $m(\mathbf{x}) = \frac{1}{d_{f_L}} \sum_{k=1}^{d_{f_L}} f_L(\mathbf{x})_k$ where d_{f_L} is the number of the nodes in the L -th layer of D_x . $\hat{m}(\hat{\mathbf{x}})$ is similarly defined for $f_L(\hat{\mathbf{x}})$. This score captures how many elements in the centered feature $f_L(\mathbf{x}) - m(\mathbf{x})$ activate together with the corresponding elements in the reconstruction $f_L(\hat{\mathbf{x}}) - \hat{m}(\hat{\mathbf{x}})$. For this score to be low, not only $a(f_L(\mathbf{x}), f_L(\hat{\mathbf{x}}))$ needs to be high but also $|m(\mathbf{x}) - \hat{m}(\hat{\mathbf{x}})|$ needs to be small. The latter term $|m(\mathbf{x}) - \hat{m}(\hat{\mathbf{x}})|$ is governed by the content loss:

Proposition 3 $|m(\mathbf{x}) - \hat{m}(\hat{\mathbf{x}})| \leq d_{f_L} \|f_L(\mathbf{x}) - f_L(\hat{\mathbf{x}})\|_1$.

Thus, if a query has a small content loss, it is reflected in the score s_a . Overall, s_a captures both the angular and content similarities between the input and its reconstruction.

Inference In the inference stage, a query \mathbf{x} is determined out-class if $s(\mathbf{x}) > \tau$ for a given threshold $\tau > 0$ and in-class otherwise. Here, the novelty score function s we use is either $s = s_c$ or $s = s_a$.

4 Experiments

In this section, we assess the effectiveness of the proposed model CSE-AE. The set of the experiments we conduct can be divided into three parts:

- (1) we test our model CSE-AE on the task of novelty detection for well-known benchmark data sets: MNIST [33], F-MNIST [65], and CIFAR-10 [31],

Table 1. Comparison of novelty detection performance on MNIST using Protocol B. **Table 2.** Comparison of novelty detection performance on F-MNIST using Protocol A.

method	AUC	method	AUC
OC-SVM [59]	0.9513	ALOCC DR [53]	0.753
KDE [5]	0.8143	ALOCC D [53]	0.601
DAE [15]	0.8766	DCAE [54]	0.908
VAE [29]	0.9696	GPND [47]	0.901
D-SVDD [50]	0.9480	OCGAN [45]	0.924
LSA [1] (CVPR'19)	0.9750	CSE-AE w/ s_c	0.929
OCGAN [45] (CVPR'19)	0.9750	CSE-AE w/ s_a	0.932
CSE-AE w/ s_c ($\alpha_z = 1.0$)	0.9669		
CSE-AE w/ s_c ($\alpha_z = 0.001$)	0.9720		
CSE-AE w/ s_a ($\alpha_z = 0.001$)	0.9752		

- (2) we examine whether our model can be successfully employed to detect adversarial examples, testing upon GTSRB stop sign dataset [61],
- (3) we conduct ablation study to carefully analyze the contribution of each component in our method.

We remark that our problem is unsupervised novelty detection. Thus, we do not compare with novelty detectors trained in other settings, for example, semi-supervised [51,23] and self-supervised [16,24] novelty detectors, which generally outperform unsupervised novelty detectors.

4.1 Novelty Detection Performance

Evaluation Protocol To assess the effectiveness of the proposed method, we test it on three well-known multi-class object recognition datasets. Following [45,1], we conduct our experiment in a one-class setting by regarding each class at a time as the known class (in-class). The network of the model is trained using only the known class samples. In the inference stage, the other remaining classes are used as out-class samples. Based on previous works tested upon the same one-class setting, we compare our method by assessing its performance using Area Under the Curve (AUC) of Receiver Operating Characteristics curve. To this end, we follow two protocols widely used in the literature [50,47,45,1] of novelty detection:

Protocol A: Given in-class and out-class sets, 80% of the in-class samples are used for training. The remaining 20% is reserved for testing. The out-class samples for testing are randomly collected from the out-class set so that its total number be equal to that of the in-class test samples.

Protocol B: We follow the training-testing splits provided from the dataset. For training, all samples in the known class in the training set are employed. For testing, all samples in the test set are used by regarding any other class as an out-class.

Table 3. Comparison of novelty detection performance on CIFAR-10 using Protocol B.

	OC-SVM [59]	KDE [5]	VAE [29]	GAN [57]	D-SVDD [50]	LSA [1]	OCGAN [45]	CSE-AE w/ s_c	CSE-AE w/ s_a
plane	0.630	0.658	0.700	0.708	0.617	0.735	0.757	0.733	0.787
car	0.440	0.520	0.386	0.458	0.659	0.580	0.531	0.657	0.737
bird	0.649	0.657	0.679	0.644	0.508	0.690	0.640	0.708	0.734
cat	0.487	0.497	0.535	0.510	0.591	0.542	0.620	0.645	0.619
deer	0.735	0.727	0.748	0.722	0.609	0.761	0.723	0.779	0.701
dog	0.500	0.496	0.523	0.505	0.657	0.546	0.620	0.680	0.722
frog	0.725	0.758	0.687	0.707	0.677	0.751	0.723	0.794	0.800
horse	0.533	0.564	0.493	0.471	0.673	0.535	0.575	0.714	0.773
ship	0.649	0.680	0.696	0.713	0.759	0.717	0.820	0.786	0.823
truck	0.509	0.540	0.386	0.458	0.731	0.548	0.554	0.6215	0.717
mean	0.5856	0.6097	0.5833	0.5916	0.6481	0.6410	0.6566	0.7117	0.7412

Datasets MNIST is composed of 70,000 handwritten digits from 0 to 9. The train/validation/test split for the dataset is 55,000/5,000/10,000.

F-MNIST is a difficult version of MNIST. The dataset has 70,000 gray scale images of fashion product from 10 categories, each category consisting of 7,000 images. The spatial size of the images is 28×28 .

CIFAR-10 CIFAR-10 consists of images from 10 different object classes. It consists of 50,000 training images and 10,000 testing images.

Architecture and hyperparameters We provide the detailed description of the architectures and hyperparameters used for our model in Supplementary Sec. 4. To briefly describe, all our networks are residual CNNs except the latent discriminator D_z , which is a multilayer perceptron with two hidden layers. To define the ensemble loss L_{eaf} , we pick f_1 from the first convolution layer and f_2, f_3 and $f_4 = f_L$ from the residual block outputs. Unless mentioned otherwise, α_x and α_z are fixed to 1.

To train the network we use Adam optimizer with $\beta_1 = 0$ and $\beta_2 = 0$. For the learning rates, we follow TTUL [25], thereby setting learning rates for (D_x, D_z) and (G, E) differently: $\text{lr}_{D_x} = \text{lr}_{D_z} = 0.0004$ and $\text{lr}_G = \text{lr}_E = 0.0001$. The input images are scaled to $[-1, 1]$. For all experiments, the total number of training iterations is 500K, which is relatively long but necessary to stabilize adversarial learning.

Results Here, we present our results together with a brief description of the hyperparameters we used.

MNIST. For MNIST dataset, we tested our model upon Protocol B. We have found that the generator of our model could learn to generate samples in the extreme (i.e., the samples near the boundary) of the in-class manifold. For this

reason, we reduced the coefficient α_z of L_{inv-z} in (6) to $\alpha_z = 0.001$, which is known to disentangle the latent code [12]. Our result is shown in Table 1, showing that the performance is comparable to the state-of-the-art model OCGAN and LSA.

F-MNIST. We assessed our model performance on F-MNIST using Protocol A. Based on the MNIST experiment, we set $\alpha_z = 0.001$. The F-MNIST dataset is not fairly easy as there is a fair amount of intra-class variation while for some classes, their inter-class dissimilarity is not so significant (for example, 'T-shirt' and 'Pullover' classes). Our result is shown in Table 2, showing that it outperforms the state-of-the-art OCGAN by a slight margin.

CIFAR-10 is typically regarded as a difficult dataset for generative modeling. Several reasons include that the dataset is fairly sparse (i.e., samples are not continuous), that it has high intra-class variation, and that the images are of low-resolution while they contain real objects. Our model shows outperforming results as shown in Table 3. We note that unlike OCGAN and GPND, our model does not apply any preprocessing on images.

4.2 Detection of Adversarial Examples

In many practical scenarios such as security systems and autonomous driving, it is vital to detect adversarial attacks [44]. In this experiment, we test our model CSE-AE on the task of adversarial example detection. Following the protocol proposed by [50], we use the 'stop sign' class of German Traffic Sign Recognition Benchmark (GTSRB) dataset [61]. The training set consists of 780 stop sign images of spatial size 32×32 . The test set is composed of 270 stop sign images and 20 adversarial examples, which are generated by applying Boundary Attack [7] on randomly drawn test stop sign images. In particular, the in-class data here is the normal stop-sign images, and the out-class instances are adversarial examples.

To train our method, we followed the same training regime, architecture, and hyperparameters as set for the above experiment over CIFAR-10. Unlike D-SVDD, we do not apply any preprocessing such as contrast normalization.

Table 4. The performance comparison over the task of detecting adversarial examples generated by Boundary Attack.

	OC-SVM	KDE	IF	AnoGAN	DCAE	D-SVDD	CSE-AE	CSE-AE
method	[59]	[5]	[35]	[57]	[54]	(ICML'18)	w/ s_a	w/ s_c
AUC	0.675	0.605	0.738	-	0.791	0.803	0.877	0.929

To measure the performance of our method over the task of adversarial example detection, we measured AUC over the test dataset. As shown in Table 4, our model performs effectively over this task. Moreover, to qualitatively assess our model, we visualized the reconstructed images of the test samples. Fig. 5 shows that our model denoises adversarial examples as it reconstructs.

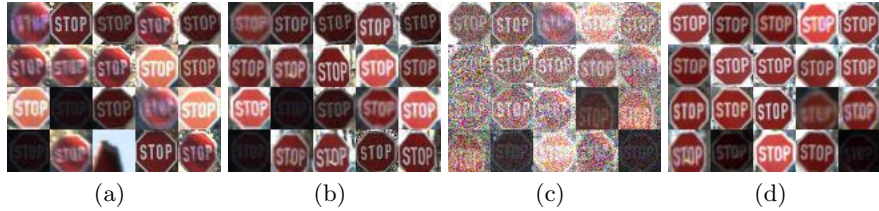


Fig. 5. Showing reconstructed images of test normal stop-sign samples and adversarial examples. (a) normal stop-sign images, (b) the reconstructions of the normal stop-sign images, (c) adversarial examples, (d) the reconstructions of the adversarial examples.

Table 5. Ablation study of the model components over CIFAR-10. Each row corresponds to each ablation model. The performance is measured in AUC.

model	$s_{per-pixel}$	s_c	s_a
AE (vanilla)	0.6067	-	-
AE w/ $L_{adv-z} + L_{adv-x}$	0.6321	0.6854	0.7080
AE w/ $L_{adv-z} + L_{adv-x} + \alpha_x L_{eaf}$	0.6472	0.6926	0.7274
full CSE-AE	0.6347	0.7117	0.7412

4.3 Ablation Study and Analysis

For all experiments below, we test upon CIFAR-10 using the same protocol used above in Sec. 4.1.

Ablation study on model components We conduct ablation study to assess the effectiveness of each component in CSE-AE. Our model can be decomposed into three parts that correspond to the adversarial loss $L_{adv-z} + L_{adv-x}$, the adversarial ensemble feature reconstruction loss L_{eaf} , and the latent reconstruction loss L_{inv-z} . According to this decomposition, we consider four models: (a) vanilla AE as a baseline (that is, the model trained with the per-pixel reconstruction loss only), (b) baseline with the adversarial loss $L_{adv-z} + L_{adv-x}$, (c) baseline with the adversarial loss plus with L_{eaf} (that is, CSE-AE without L_{inv-z}), (d) full CSE-AE. To measure the reconstruction error for each model, we employ three different novelty scores: (i) the score by the conventional per-pixel reconstruction error

$$s_{per-pixel}(x) := \|\mathbf{x} - \hat{\mathbf{x}}\|_1, \quad (10)$$

(ii) the score by the content reconstruction loss $s_c(\mathbf{x})$ defined in Eq. (8), and (iii) the centered co-activation novelty score $s_a(\mathbf{x})$.

The results in Table 5 show that each component of our method contributes to improving the novelty detection performance.

On ensembled adversarial features The ensemble loss L_{eaf} in (5) has been analyzed by varying the number L of ensemble components. We note that the

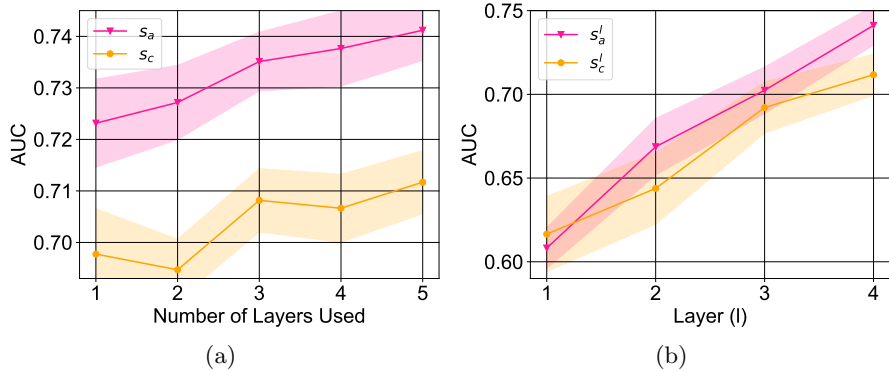


Fig. 6. The novelty detection performances of CSE-AE by (a) varying L in L_{leaf} and (b) varying L in $s_c(\mathbf{x})$ and $s_a(\mathbf{x})$, respectively.

final layer f_L is always used for all cases. The AUC performance is measured using each of the novelty scores s_c and s_a . The results in Fig. 6 (a) show that the performance improves as we use larger L for L_{leaf} .

Choice of feature layer for novelty score We experimentally studied how the novelty detection performance changes as we define the novelty score by another feature layer f_l in D_x with $l < L$. Specifically, we replaced the score $s_c(\mathbf{x})$ in (8) by

$$s_c^l(\mathbf{x}) = \|f_l(\mathbf{x}) - f_l(\hat{\mathbf{x}})\|_1, \quad (11)$$

and similarly $s_a(\mathbf{x})$ by

$$s_a^l(\mathbf{x}) = 1 - a(f_l(\mathbf{x}) - m(\mathbf{x}), f_l(\hat{\mathbf{x}}) - \hat{m}(\hat{\mathbf{x}})). \quad (12)$$

The comparison is shown in Fig. 6 (b), depicting a clear sign of monotonicity between the performance and the layer depth l .

5 Conclusion

In this paper, we have proposed a novel autoencoder framework CSE-AE for unsupervised novelty detection, and introduced techniques to effectively realize the framework. In our realization of CSE-AE, the encoding of an arbitrary input is constrained into a compact manifold by exploiting both GAN and DNN’s ignorance of the unknown. Concurrently, adversarially training the decoder induces the encoder to surjectively map the in-class data to the compact manifold while the ensembled reconstruction losses ensure the fine reconstruction of in-class data. Overall, the realized CSE-AE effectively achieves to reconstruct the in-class data finely and out-class poorly. Moreover, similarity metrics based on the penultimate features from the input discriminator have been successfully employed to aptly differentiate the reconstruction discrepancy over the in-class from that over out-class.

References

1. Abati, D., Porrello, A., Calderara, S., Cucchiara, R.: Latent space autoregression for novelty detection. In: Proceedings of the IEEE Conference on Computer Vision and Pattern Recognition. pp. 481–490 (2019)
2. Adam, A., Rivlin, E., Shimshoni, I., Reinitz, D.: Robust real-time unusual event detection using multiple fixed-location monitors. *IEEE transactions on pattern analysis and machine intelligence* **30**(3), 555–560 (2008)
3. An, J., Cho, S.: Variational autoencoder based anomaly detection using reconstruction probability. *Special Lecture on IE* **2**(1) (2015)
4. Bengio, Y., Courville, A., Vincent, P.: Representation learning: A review and new perspectives. *IEEE transactions on pattern analysis and machine intelligence* **35**(8), 1798–1828 (2013)
5. Bishop, C.M.: *Pattern recognition and machine learning*. Springer Science+ Business Media (2006)
6. Boulton, T., Cruz, S., Dhamija, A., Gunther, M., Henrydoss, J., Scheirer, W.: Learning and the unknown: Surveying steps toward open world recognition. In: Proceedings of the AAAI Conference on Artificial Intelligence. vol. 33, pp. 9801–9807 (2019)
7. Brendel, W., Rauber, J., Bethge, M.: Decision-based adversarial attacks: Reliable attacks against black-box machine learning models. *arXiv preprint arXiv:1712.04248* (2017)
8. Candès, E.J., Li, X., Ma, Y., Wright, J.: Robust principal component analysis? *Journal of the ACM (JACM)* **58**(3), 11 (2011)
9. Chalapathy, R., Menon, A.K., Chawla, S.: Robust, deep and inductive anomaly detection. In: *Joint European Conference on Machine Learning and Knowledge Discovery in Databases*. pp. 36–51. Springer (2017)
10. Chandola, V., Banerjee, A., Kumar, V.: Anomaly detection: A survey. *ACM Comput. Surv.* **41**(3), 15:1–15:58 (Jul 2009). <https://doi.org/10.1145/1541880.1541882>, <http://doi.acm.org/10.1145/1541880.1541882>
11. Chen, J., Sathe, S., Aggarwal, C., Turaga, D.: Outlier detection with autoencoder ensembles. In: *Proceedings of the 2017 SIAM International Conference on Data Mining*. pp. 90–98. SIAM (2017)
12. Chen, X., Duan, Y., Houthoofd, R., Schulman, J., Sutskever, I., Abbeel, P.: Infogan: Interpretable representation learning by information maximizing generative adversarial nets. In: *Advances in neural information processing systems*. pp. 2172–2180 (2016)
13. Cong, Y., Yuan, J., Liu, J.: Sparse reconstruction cost for abnormal event detection. In: *CVPR 2011*. pp. 3449–3456. IEEE (2011)
14. Duncan, K., Ketz, N., Inati, S.J., Davachi, L.: Evidence for area cal as a match/mismatch detector: A high-resolution fmri study of the human hippocampus. *Hippocampus* **22**(3), 389–398 (2012)
15. El-Yaniv, R., Nisenson, M.: Optimal single-class classification strategies. In: *Advances in Neural Information Processing Systems*. pp. 377–384 (2007)
16. Golan, I., El-Yaniv, R.: Deep anomaly detection using geometric transformations. In: *Advances in Neural Information Processing Systems*. pp. 9758–9769 (2018)
17. Goodfellow, I., Pouget-Abadie, J., Mirza, M., Xu, B., Warde-Farley, D., Ozair, S., Courville, A., Bengio, Y.: Generative adversarial nets. In: *Advances in neural information processing systems*. pp. 2672–2680 (2014)

18. Gretton, A., Borgwardt, K.M., Rasch, M.J., Schölkopf, B., Smola, A.: A kernel two-sample test. *Journal of Machine Learning Research* **13**(Mar), 723–773 (2012)
19. Guha, S., Mishra, N., Roy, G., Schrijvers, O.: Robust random cut forest based anomaly detection on streams. In: *International conference on machine learning*. pp. 2712–2721 (2016)
20. Hadsell, R., Chopra, S., LeCun, Y.: Dimensionality reduction by learning an invariant mapping. In: *2006 IEEE Computer Society Conference on Computer Vision and Pattern Recognition (CVPR'06)*. vol. 2, pp. 1735–1742. IEEE (2006)
21. He, K., Zhang, X., Ren, S., Sun, J.: Deep residual learning for image recognition. In: *Proceedings of the IEEE conference on computer vision and pattern recognition*. pp. 770–778 (2016)
22. Hendrycks, D., Gimpel, K.: A baseline for detecting misclassified and out-of-distribution examples in neural networks. *arXiv preprint arXiv:1610.02136* (2016)
23. Hendrycks, D., Mazeika, M., Dietterich, T.: Deep anomaly detection with outlier exposure. *arXiv preprint arXiv:1812.04606* (2018)
24. Hendrycks, D., Mazeika, M., Kadavath, S., Song, D.: Using self-supervised learning can improve model robustness and uncertainty. In: *Advances in Neural Information Processing Systems*. pp. 15637–15648 (2019)
25. Heusel, M., Ramsauer, H., Unterthiner, T., Nessler, B., Hochreiter, S.: Gans trained by a two time-scale update rule converge to a local nash equilibrium. In: *Advances in Neural Information Processing Systems*. pp. 6626–6637 (2017)
26. Hoffmann, H.: Kernel pca for novelty detection. *Pattern recognition* **40**(3), 863–874 (2007)
27. Johnson, J., Alahi, A., Fei-Fei, L.: Perceptual losses for real-time style transfer and super-resolution. In: *European conference on computer vision*. pp. 694–711. Springer (2016)
28. Kim, J., Grauman, K.: Observe locally, infer globally: a space-time mrf for detecting abnormal activities with incremental updates. In: *2009 IEEE Conference on Computer Vision and Pattern Recognition*. pp. 2921–2928. IEEE (2009)
29. Kingma, D.P., Welling, M.: Auto-encoding variational bayes. *arXiv preprint arXiv:1312.6114* (2013)
30. Knight, R.T.: Contribution of human hippocampal region to novelty detection. *Nature* **383**(6597), 256 (1996)
31. Krizhevsky, A., Hinton, G., et al.: Learning multiple layers of features from tiny images. *Tech. rep., Citeseer* (2009)
32. Krizhevsky, A., Sutskever, I., Hinton, G.E.: Imagenet classification with deep convolutional neural networks. In: *Advances in neural information processing systems*. pp. 1097–1105 (2012)
33. LeCun, Y., Cortes, C.: MNIST handwritten digit database (2010), <http://yann.lecun.com/exdb/mnist/>
34. Lee, K., Lee, H., Lee, K., Shin, J.: Training confidence-calibrated classifiers for detecting out-of-distribution samples. *arXiv preprint arXiv:1711.09325* (2017)
35. Liu, F.T., Ting, K.M., Zhou, Z.H.: Isolation forest. In: *2008 Eighth IEEE International Conference on Data Mining*. pp. 413–422. IEEE (2008)
36. Mahadevan, V., Li, W., Bhalodia, V., Vasconcelos, N.: Anomaly detection in crowded scenes. In: *2010 IEEE Computer Society Conference on Computer Vision and Pattern Recognition*. pp. 1975–1981. IEEE (2010)
37. Makhzani, A., Shlens, J., Jaitly, N., Goodfellow, I., Frey, B.: Adversarial autoencoders. *arXiv preprint arXiv:1511.05644* (2015)
38. Miyato, T., Kataoka, T., Koyama, M., Yoshida, Y.: Spectral normalization for generative adversarial networks. *arXiv preprint arXiv:1802.05957* (2018)

39. Moosavi-Dezfooli, S.M., Fawzi, A., Fawzi, O., Frossard, P.: Universal adversarial perturbations. In: Proceedings of the IEEE conference on computer vision and pattern recognition. pp. 1765–1773 (2017)
40. Nalisnick, E., Matsukawa, A., Teh, Y.W., Gorur, D., Lakshminarayanan, B.: Do deep generative models know what they don't know? arXiv preprint arXiv:1810.09136 (2018)
41. Nguyen, H.V., Bai, L.: Cosine similarity metric learning for face verification. In: Asian conference on computer vision. pp. 709–720. Springer (2010)
42. Oza, P., Patel, V.M.: One-class convolutional neural network. *IEEE Signal Processing Letters* **26**(2), 277–281 (2018)
43. Oza, P., Patel, V.M.: Active authentication using an autoencoder regularized cnn-based one-class classifier. arXiv preprint arXiv:1903.01031 (2019)
44. Papernot, N., McDaniel, P., Goodfellow, I., Jha, S., Celik, Z.B., Swami, A.: Practical black-box attacks against machine learning. In: Proceedings of the 2017 ACM on Asia conference on computer and communications security. pp. 506–519. ACM (2017)
45. Perera, P., Nallapati, R., Xiang, B.: Ocgan: One-class novelty detection using gans with constrained latent representations. In: Proceedings of the IEEE Conference on Computer Vision and Pattern Recognition. pp. 2898–2906 (2019)
46. Perera, P., Patel, V.M.: Dual-minimax probability machines for one-class mobile active authentication. In: 2018 IEEE 9th International Conference on Biometrics Theory, Applications and Systems (BTAS). pp. 1–8. IEEE (2018)
47. Pidhorskyi, S., Almohsen, R., Doretto, G.: Generative probabilistic novelty detection with adversarial autoencoders. In: Advances in Neural Information Processing Systems. pp. 6822–6833 (2018)
48. Pimentel, M.A., Clifton, D.A., Clifton, L., Tarassenko, L.: A review of novelty detection. *Signal Processing* **99**, 215–249 (2014)
49. Roberts, S.J.: Novelty detection using extreme value statistics. *IEE Proceedings-Vision, Image and Signal Processing* **146**(3), 124–129 (1999)
50. Ruff, L., Vandermeulen, R., Goernitz, N., Deecke, L., Siddiqui, S.A., Binder, A., Müller, E., Kloft, M.: Deep one-class classification. In: International Conference on Machine Learning. pp. 4393–4402 (2018)
51. Ruff, L., Vandermeulen, R.A., Görnitz, N., Binder, A., Müller, E., Müller, K.R., Kloft, M.: Deep semi-supervised anomaly detection. arXiv preprint arXiv:1906.02694 (2019)
52. Sabokrou, M., Fayyaz, M., Fathy, M., Moayed, Z., Klette, R.: Deep-anomaly: Fully convolutional neural network for fast anomaly detection in crowded scenes. *Computer Vision and Image Understanding* **172**, 88–97 (2018)
53. Sabokrou, M., Khalooei, M., Fathy, M., Adeli, E.: Adversarially learned one-class classifier for novelty detection. In: Proceedings of the IEEE Conference on Computer Vision and Pattern Recognition. pp. 3379–3388 (2018)
54. Sakurada, M., Yairi, T.: Anomaly detection using autoencoders with nonlinear dimensionality reduction. In: Proceedings of the MLSDA 2014 2nd Workshop on Machine Learning for Sensory Data Analysis. p. 4. ACM (2014)
55. Saleh, B., Farhadi, A., Elgammal, A.: Object-centric anomaly detection by attribute-based reasoning. In: Proceedings of the IEEE Conference on Computer Vision and Pattern Recognition. pp. 787–794 (2013)
56. Schlegl, T., Seeböck, P., Waldstein, S.M., Langs, G., Schmidt-Erfurth, U.: f-anogan: Fast unsupervised anomaly detection with generative adversarial networks. *Medical image analysis* **54**, 30–44 (2019)

57. Schlegl, T., Seeböck, P., Waldstein, S.M., Schmidt-Erfurth, U., Langs, G.: Unsupervised anomaly detection with generative adversarial networks to guide marker discovery. In: International Conference on Information Processing in Medical Imaging. pp. 146–157. Springer (2017)
58. Schölkopf, B., Platt, J.C., Shawe-Taylor, J.C., Smola, A.J., Williamson, R.C.: Estimating the support of a high-dimensional distribution. *Neural Comput.* **13**(7), 1443–1471 (Jul 2001). <https://doi.org/10.1162/089976601750264965>, <https://doi.org/10.1162/089976601750264965>
59. Schölkopf, B., Williamson, R.C., Smola, A.J., Shawe-Taylor, J., Platt, J.C.: Support vector method for novelty detection. In: Advances in neural information processing systems. pp. 582–588 (2000)
60. Sokolov, E.N.: Higher nervous functions: The orienting reflex. *Annual review of physiology* **25**(1), 545–580 (1963)
61. Stallkamp, J., Schlipsing, M., Salmen, J., Igel, C.: The german traffic sign recognition benchmark: A multi-class classification competition. In: *IJCNN*. vol. 6, p. 7 (2011)
62. Tiitinen, H., May, P., Reinikainen, K., Näätänen, R.: Attentive novelty detection in humans is governed by pre-attentive sensory memory. *Nature* **372**(6501), 90 (1994)
63. Wang, F., Xiang, X., Cheng, J., Yuille, A.L.: Normface: L2 hypersphere embedding for face verification. In: Proceedings of the 25th ACM international conference on Multimedia. pp. 1041–1049 (2017)
64. Wen, Y., Zhang, K., Li, Z., Qiao, Y.: A discriminative feature learning approach for deep face recognition. In: European conference on computer vision. pp. 499–515. Springer (2016)
65. Xiao, H., Rasul, K., Vollgraf, R.: Fashion-mnist: a novel image dataset for benchmarking machine learning algorithms. *arXiv preprint arXiv:1708.07747* (2017)
66. Yosinski, J., Clune, J., Nguyen, A., Fuchs, T., Lipson, H.: Understanding neural networks through deep visualization. *arXiv preprint arXiv:1506.06579* (2015)
67. Zeiler, M.D., Fergus, R.: Visualizing and understanding convolutional networks. In: European conference on computer vision. pp. 818–833. Springer (2014)
68. Zhang, R., Isola, P., Efros, A.A., Shechtman, E., Wang, O.: The unreasonable effectiveness of deep features as a perceptual metric. In: Proceedings of the IEEE Conference on Computer Vision and Pattern Recognition. pp. 586–595 (2018)
69. Zhao, B., Fei-Fei, L., Xing, E.P.: Online detection of unusual events in videos via dynamic sparse coding. In: *CVPR 2011*. pp. 3313–3320. IEEE (2011)
70. Zheng, P., Yuan, S., Wu, X., Li, J., Lu, A.: One-class adversarial nets for fraud detection. In: Proceedings of the AAAI Conference on Artificial Intelligence. vol. 33, pp. 1286–1293 (2019)
71. Zhu, J.Y., Park, T., Isola, P., Efros, A.A.: Unpaired image-to-image translation using cycle-consistent adversarial networks. In: Proceedings of the IEEE international conference on computer vision. pp. 2223–2232 (2017)